An Understanding of the X-ray Absorption Near-Edge Structure of Copper(II) Imidazole Complexes

R. W. Strange,[†,§] L. Alagna,[‡] P. Durham,[†] and S. S. Hasnain*[,†]

Contribution from the Daresbury Laboratory, Warrington, WA4 4AD, UK, Consiglio Nazionale delle Ricerche, I-00016 Montrotondo Stazione, Roma, Italy, and Chemistry Department, Manchester University, Manchester, M13 9PL, UK. *Received July 31, 1989*

Abstract: Detailed multiple scattering calculations have been carried out to understand the K-edge X-ray absorption near-edge structure (XANES) of a number of copper(II) imidazole compounds. Results are presented which show that each of the spectral features observed in the XANES can be understood as arising primarily from electron-scattering effects. The calculations suggest that contributions to the XANES from secondary processes (e.g., "shake-off" effects) are negligible. Evidence is presented for the existence of electron scattering between the imidazole ligands.

Over the past 12 years extended X-ray absorption fine structure (EXAFS) has provided structural information on a number of metalloproteins.[1-4] However, these studies have provided no or limited information about the geometrical arrangement of the ligands around the metal atoms due to the predominantly single scattering nature of the EXAFS. Even though it has long been realized that such detailed stereochemical information is present in the strong scattering region near the absorption edge (X-ray absorption near edge structure or XANES), only limited use has been made of this part of the X-ray absorption spectrum due to the computational complexity involved. Recently, several theoretical approaches have been developed to explain the details of the XANES spectrum.[5,6]

The structural features present in the XANES spectrum may arise, in general, from a number of one- or multielectron processes that modulate the atomic absorption. These processes include bound state transitions from the core state to empty valence states, "shake-up"-"shake-down" transitions, and continuum resonances involving backscattering of the excited photoelectron by the atomic potentials surrounding the absorbing atom. In this work we concentrate on the latter process, where strong multiple scattering is present due to the long mean free path of the excited photoelectron at low energies. We have used the one-electron multiple-scattering approach developed by Durham et al.[5] to study the XANES of a number of Cu(II) imidazole complexes. This approach has previously been successful in its attempt to explain the XANES spectra of complex biological systems like hemoproteins.[7-9] Our aim has been to understand and to clarify the contributions to the XANES of these Cu(II) systems that arise solely from the continuum resonances. We discuss the possibility of extending this treatment to obtain detailed stereochemical information about the metal sites in noncrystalline proteins and proteins in solution, having established the nature and distance of ligands from the crystallographic and EXAFS data.

Materials and Methods

XANES spectra were measured from powder samples of the Cu(II) imidazole complexes by using the transmission mode facilities on station 7.1 at the SRS, Daresbury Laboratory. The maximum beam current was 200 mA at 2 GeV. A Si(111) double crystal order-sorting monochromator was used to reduce the harmonic content of the monochromatic beam. The monochromator was calibrated in energy space by setting the maximum of the first feature in the absorption edge of metallic Cu foil to 8982 eV. Experimental details for measurement of the XANES of aqueous superoxide dismutase have been described elsewhere.[10] Established procedures were used to calibrate and normalize the absorption data.[11]

Atomic phase shifts were calculated within the muffin-tin approximation by using Clementi—Roetti wave functions.[12] Nonoverlapping muffin-tin radii were constructed by using the structure of tetrakis(imidazole)copper(II) nitrate[13] as a model. Exchange and correlation effects were included in the calculation, and the excited Cu atom was represented by the wave functions of a neutral (Z + 1) atom, where the occupancy of the 1s orbital is reduced by one.

Theoretical calculations of the XANES were performed by using the multiple scattering computational scheme developed by Durham et al.,[5] including one shell of atoms at a time up to three shells, with a maximum of 22 atoms. Calculations were performed within the dipolar approximation for both $m_l = \pm 1$ and $m_l = 0$ final states. The weighted average of these two components compares to the experimental XANES obtained from a polycrystalline sample. The calculations were based on a minor simplification of the crystal structure coordinates for the complexes studied. This was done in order to exploit the symmetry properties of the resulting structures, thus reducing the computation time by at least an order of magnitude. Computations were performed with an FPS-164 processor attached to an AS-7000 mainframe, with a maximum run time of about 10 min.

Results and Discussion

An Understanding of the Spectral Features. Figure 1 shows the experimental XANES for three imidazole complexes each with two axial ligands to the CuN_4 plane. Also shown is the spectrum for the Cu site of superoxide dismutase in aqueous solution. In each of the chemical systems, Cu is ligated to four imidazole groups with two weakly coordinating axial ligands. In the case of the enzyme, Cu is known to be coordinated to four histidine imidazole groups and a water molecule at 2.24 Å. The close similarity of the ligands and their distances is reflected in the similar nature of the XANES profile which the four systems display. However, the XANES spectra show features with varying

[†] Daresbury Laboratory.
[‡] Consiglio Nazionale dell Ricerche.
[§] Manchester University.

(1) Powers L. *Biophys. Acta* **1982**, *683*, 1.
(2) *EXAFS and Near Edge Structure*; Bianconi, A., Incoccia, L., Stipcich, S., Eds.; Springer-Verlag: Berlin, 1983.
(3) EXAFS and Near Edge Structure III; Hodgson, K. O., Hedman, B., Penner-Hahn, J. E., Eds.; Springer-Verlag: Berlin, 1984.
(4) *EXAFS and Near Edge Structure IV*; Lagarde, P., Raoux, D., Petiau, J., Eds.; J. de Phys.; Colloque C8, 47, 1986; Vols. 1 and 2.
(5) Durham, P. J.; Pendry, J. B.; Hodges, C. H. *Comput. Phys. Commun.* **1982**, *25*, 193.
(6) (a) Natoli, C. R.; Misemer, D. K.; Doniach, S.; Kutzler, F. W. *Phys. Rev* **1980**, *22a*, 1104. (b) Kutzler, F. W.; Natoli, C. R.; Misemer, D. K.; Doniach, S.; Hodgson, K. O. *J. Chem. Phys.* **1980**, *73*, 3274-3288.
(7) Durham, P. J.; Bianconi, A.; Congiu-Castellano, A.; Giovanelli, A.; Hasnain, S. S.; Incoccia, L.; Morante, S.; Pendry, J. B. *EMBO* **1983**, *2*, 1441.
(8) Bianconi, A.; Congiu-Castellano, A.; Dell'Ariccia, M.; Giovanelli, A.; Buratteni, E.; Castagnola, M.; Durham, P. J. *Biochem. Biophys. Acta* **1985**, *831*, 120.
(9) Bianconi, A.; Congiu-Castellano, A.; Durham, P. J.; Hasnain, S. S.; Phillips, S. *Nature* **1985**, *318*, 685.
(10) (a) Blackburn, N. J.; Hasnain, S. S.; Diakun, G. P.; Knowles, P. F.; Binsted, N.; Garner, C. D *Biochem. J.* **1983**, *213*, 765. (b) Blackburn, N. J.; Hasnain, S. S.; Incoccia, L.; Morante, S.; Pendry, J. B. *EMBO* **1983**, *2*, 1441. (c) Blackburn, N. J.; Hasnain, S. S.; Binsted, N.; Diakun, G. P.; Garner, C. D.; Knowles, P. F. *Biochem. J.* **1984**, *219*, 985. (c) Blackburn, N. J.; Strange, R. W.; McFadden, L. M.; Hasnain, S. S. *J. Am. Chem. Soc.* **1987**, *109*, 7162.
(11) E.g., Pantos, E. Daresbury Laboratory, 1982, Preprint DL/SCI/P346E.
(12) Clementi, E., Roetti, C. *Atomic Data and Nuclear Data Tables*; Academic Press: New York, 1974; Vol. 14, No. 3-4.
(13) McFadden, D. L.; McPhail, A. T.; Garner, C. D.; Mabbs, F. E. *J. Chem. Soc., Dalton Trans.* **1976**, 47-52.

0002-7863/90/1512-4265$02.50/0

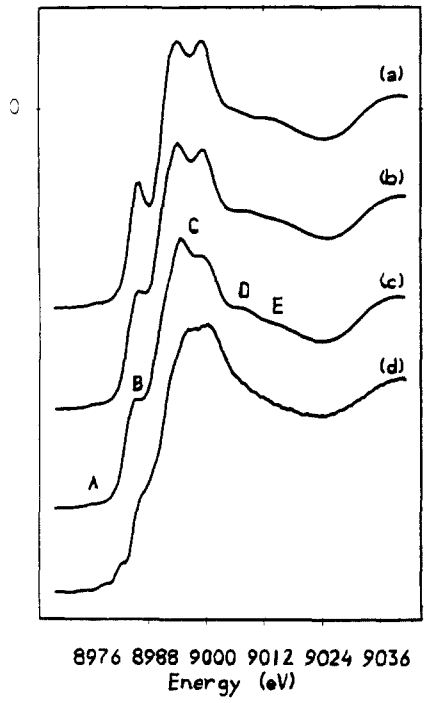

Figure 1. Copper K-edge absorption spectra for (a) tetrakis(imidazole)copper(II) nitrate; (b) tetrakis(imidazole)copper(II) perchlorate; (c) tetrakis(methylimidazole)copper(II) boron tetrafluoride; and (d) native superoxide dismutase.

degrees of resolution, suggesting significant stereochemical differences between them. As we will see in the following sections, each of these features, their relative intensity, and resolution are a signature of a particular aspect of the structure.

The features labeled A–E in Figure 1 have previously been assigned to various origins. Feature A (~8979 eV) has been identified as originating from a 1s → 3d quadrupolar allowed transition,[14] and this has recently been confirmed by single-crystal polarized XANES studies.[15] The origin of feature B (~8986 eV) is less certain and has been suggested as arising from either a vibronically allowed 1s → 4s transition,[16] a 1s → 4p simultaneous with ligand-to-metal shake-down,[17,18] or as a 1s → 4p transition.[19] The feature labeled C (~8990–9000 eV) has been assigned as a 1s → 4p[18] or as a 1s → continuum resonance.[19] The features D and E (>9000 eV) have generally been understood as arising from continuum resonances involving multiple-scattering effects. In the present work we show that all the features of the XANES from B to E depend upon the detailed geometry of the Cu(II) coordination sphere to ~4.2 Å, and thus an explanation based upon scattering theory may be more appropriate. For example, the peak marked B arises primarily due to scattering by the axial ligands; its intensity and position is related to the number and position of these ligands. Similarly, features D and E depend upon the orientation of the imidazole rings with respect to the CuN_4 plane.

Figure 2a shows the scattering contribution with four nitrogens in a square-planar arrangement at an average distance of 2.01 Å. Calculations are shown in which the photon polarization is normal (n) or parallel (p) to the plane of the four nitrogen nearest neighbors; naturally the p-component of the spectrum is sensitive to scattering events within the plane, while the scattering by the

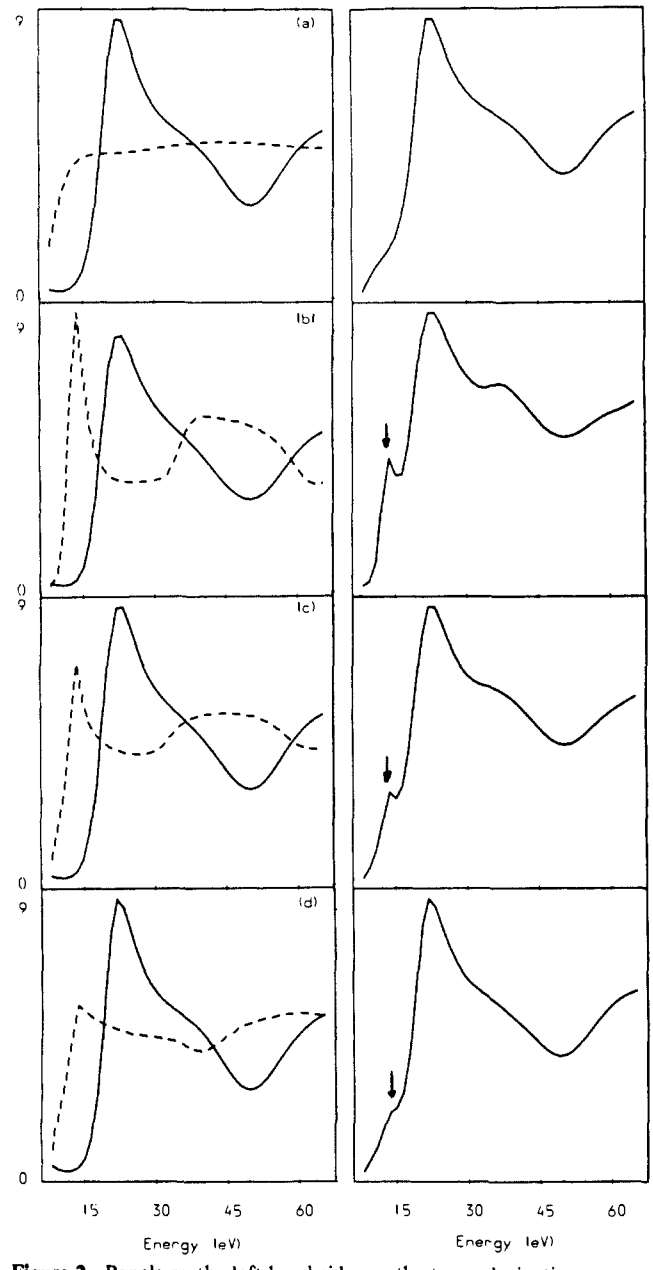

Figure 2. Panels on the left hand side are the two polarization components, p (solid curve) and n (dashed curve). Right hand panels give the averaged spectrum: (a) one-shell calculation for a CuN_4 unit, where Cu–N distances are 2.01 Å; (b) calculations with a CuN_4O_2 unit, where oxygen atoms are placed at 2.56 Å normal to the CuN_4 plane (the arrowed feature corresponds to experimental feature B in Figure 1); (c) calculations for a CuN_4O unit, where a single oxygen atom is at 2.56 Å; (d) same as (c) but with the axial oxygen at 2.24 Å.

axial ligands shows up most in the n-component. The polarization-averaged spectrum is shown in the right hand panel. Figure 2b–d shows the effect of the axial ligands. As expected, the parallel (i.e., in-plane) contribution is not affected, but a sharp resonance near the onset of photoabsorption appears in the n-component. Figure 2b shows these contributions with two axial oxygen ligands included at 2.56 Å. The main contribution, marked with an arrow, due to these axial ligands results in a well-defined peak in the averaged spectrum. The position of this contribution and peak remains unchanged when the calculations are done with only one axial ligand at the same distance (Figure 2c). However, due to the weaker scattering contribution from one axial ligand compared to two axial ligands, the intensity of this peak is reduced. The effect of the position of the axial ligand is shown in Figure 2d which shows the individual n- and p-components and the average. These calculations are based on a CuN_4O unit with the axial oxygen at 2.24 Å, a distance determined from the EXAFS study

(14) Schulman, R. G.; Yafet, T.; Eisenberger, P.; Blumberg, W. E. *em PNAS* **1976**, *73*, 1384.
(15) Hahn, J. E.; Scott, R. A.; Hodgson, K. O.; Doniach, S.; Desjardins, S. E.; Solomon, E. I. *Chem. Phys. Lett.* **1982**, *88*, 595.
(16) Chan, S. I.; Hu, V. W.; Gamble, R. C. *J. Mol. Struct.* **1978**, *45*, 239.
(17) Blair, R. A.; Goddard, W. A. *Phys. Rev.* **1980**, *b22*, 2767.
(18) (a) Kosugi, N.; Yokoyama, T.; Asakura, K.; Kuroda, H. *Chem. Phys.* **1984**, *91*, 249.; (b) Yokoyama, T.; Kosugi, N.; Kuroda, H. *Chem. Phys.* **1986**, *103*, 101.
(19) Smith, T. A.; Berding, M.; Penner-Hahn, J. E.; Doniach, S.; Hodgson, K. O. *J. Am. Chem. Soc.* **1985**, *107*, 5945.

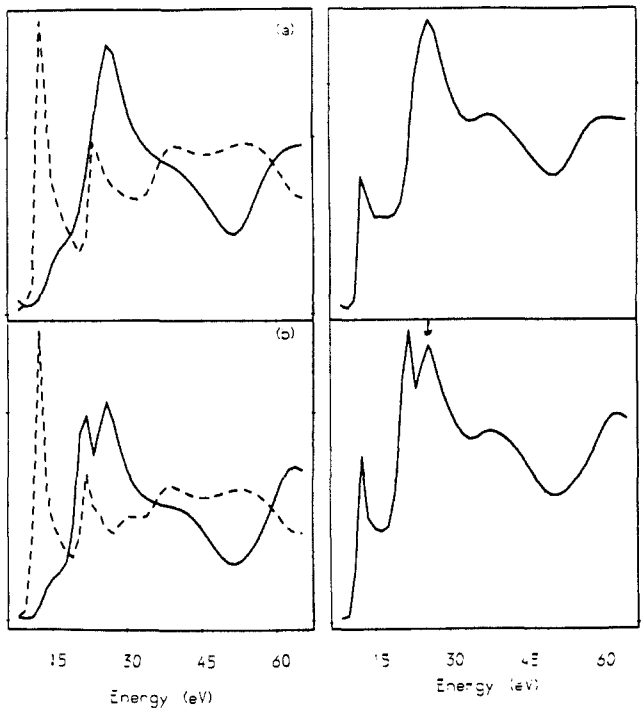

Figure 3. (a) Calculations for a $CuN_4C_8O_2$ unit, i.e.; eight carbons from the imidazole rings are included and (b) calculations incorporating all the atoms of the imidazole rings. All four rings are oriented perpendicular to the CuN_4 plane. The peak marked by an arrow is predominantly due to scattering from the third shell atoms.

of superoxide dismutase. Thus, a comparison of these simple one-shell calculations allows us to establish that the peak marked "B" in the experimental spectrum arises primarily from the axial ligands and that the observed difference in the Cu(II) complexes and the protein is partly due to a reduction in the number of axial ligands and its position (Figure 2 (parts b and d)). This is consistent with the EXAFS result of superoxide dismutase[10] which shows that the axial oxygen atom is at 2.24 Å, compared to the two oxygen atoms in a chemical system such as $Cu(imid)_4(NO_3)_2$, which are at an average distance of 2.56 Å.[13] These calculations are in qualitative agreement with the multiple scattering X_α calculations reported by Smith et al. (see Figure 7a in ref 19) and with the recent results of Onori et al.[20]

The effect of the second shell of eight carbons (from the four imidazole rings) and third shell of four nitrogens and four carbons is shown in Figure 3 (parts a and b). These additional atoms are arranged such that the imidazole rings are oriented perpendicular to the CuN_4 plane. A comparison of Figure 3a with Figure 2b shows the increased resolution of the photothreshold feature (~11 eV) and the increased intensity of the white line (~27 eV) with the inclusion of the second shell of carbon atoms. The calculation with the third shell of atoms, i.e., the remaining carbon and nitrogen atoms of the imidazole rings, results in a well-resolved doublet at ~20–27 eV in the averaged spectrum.

In order to assess the presence of orientation dependence for the XANES features, calculations were also made with a geometry in which two of the imidazole rings are oriented perpendicular and two parallel to the CnN_4 plane. The averaged spectrum for this calculation is shown in Figure 4a, where it is compared with the previous calculation with all four rings perpendicular (Figure 3b). The main differences between these two cases lies in the region we have marked D and E in the experimental spectra (Figure 1). Changing the relative orientation of the rings also affect the peak (B) primarily contributed by the axial ligands. This is not surprising as the scattering from the outer shell atoms affects its position. These results are all reflected in recent experimental data obtained for two crystal forms[21] of Cu(methylimidazole)$_4$(BF$_4$)$_2$. Figure 4b shows the experimental data for the monoclinic and tetragonal forms of this complex. In the monoclinic form, which corresponds to the calculation with two rings parallel and two perpendicular to the CuN_4 plane, features D and E are both present. In the tetragonal form, where all four rings are nearly perpendicular to the CuN_4 plane, only a single feature is observed, as in the calculations. In this case the feature B is more intense and sharper; also the relative intensity of the doublet C changes in accordance with the calculations. Essentially all the features of the experimental spectra are reproduced by the calculations. This, we believe, provides a clear demonstration that the XANES of these complexes can be understood primarily by electron-scattering calculations.

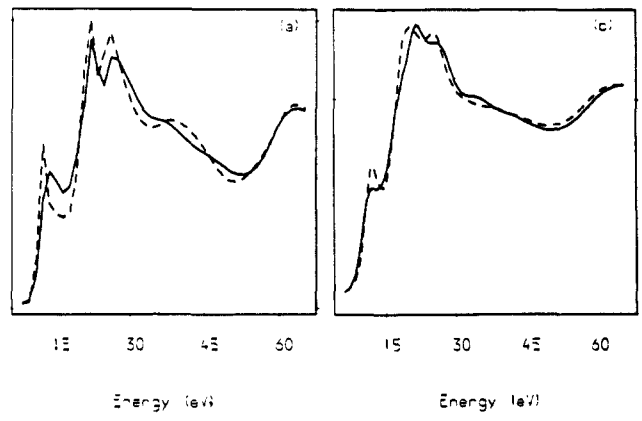

Figure 4. a) A comparison of two theoretical spectra. The dashed curve is the calculation with all four imidazole rings oriented perpendicular to the CuN_4 plane; the solid curve is the calculation with two rings perpendicular and two rings parallel to the CuN_4 plane. (b) A comparison of two experimental spectra. The dashed curve is the XANES of tetragonal $Cu(meim)_4(BF_4)_2$, where the four rings are perpendicular to the CuN_4 plane, and the solid curve is the XANES of monoclinic $Cu(meim)_4(BF_4)_2$, where two rings are perpendicular and two rings are parallel to the CuN_4 plane.

The sensitivity of the XANES spectra to relative ring orientation may only be a reflection of the number of atoms contributing to the n- or p-polarization. However, an intriguing possibility is whether there may be contributions to the XANES from "inter-ring" scattering effects. We have examined this possibility by carrying out multiple-scattering calculations for a number of geometries in which only two imidazole rings participate, with the axial ligands excluded. These calculation were for the following ring orientations: both rings perpendicular to the xy plane, with the rings positioned along the x and $-x$ axes I and with the rings along the x and y axes II; both rings parallel to the xy plane, with the rings positioned along the x and $-x$ axes III and with the rings along the x and y axes IV; and one ring perpendicular to the xy plane and one ring parallel to the xy plane, with the rings positioned along the x and $-x$ axes V and with the rings along the x and y axes VI.

Figure 5 shows comparisons between calculations I and II (Figure 5a), III and IV (Figure 5b), II and VI (Figure 5c), and V and VI (Figure 5d).

There is clear evidence in these calculations for the presence of "inter-ring" scattering. In particular, each of the pairs of spectra shown in Figure 5 (parts a, b, and d) should be identical in the absence of "inter-ring" scattering contributions. In each case the effect shows up mostly in the p-component of the polarization and is more significant when the atoms of the two rings are in closer proximity, as is the case for the dashed curves in Figure 5 (parts a and b).

The calculations shown in Figure 5c are based on the two geometries relevant to the experimental situation. Both the n- and p-components of the polarization are affected in this case due to the change in the number of atoms contributing to the xy polarization. The main difference between the two averaged

(20) Onori, G.; Santucci, A.; Scafati, A.; Belli, M.; Della Longa, S.; Bianconi, A. *Chem. Phys. Lett.* **1988**, *149*, 289–294.

(21) Collison, C. D.; Garner, C. D. Unpublished results.

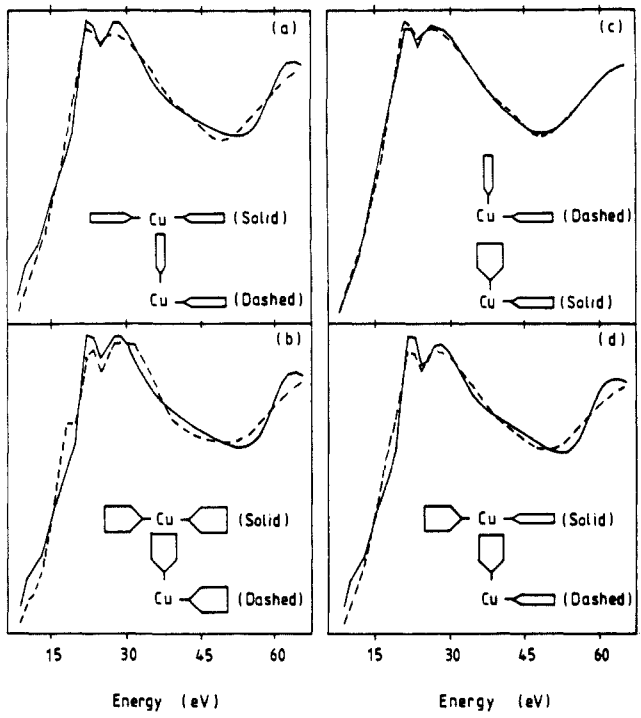

Figure 5. This shows a series of calculations involving only two imidazole rings. The relative orientation of the rings is varied as indicated in the figure.

calculations (Figure 5c) is at the position marked by an arrow, which corresponds to the region we have labeled D and E in the experimental data (Figure 1). This difference is enhanced when all four rings are present, as shown in Figure 4a, and the evidence suggests that it is due to "inter-ring" scattering. In other words, the electron is scattered between adjacent ring atoms before being backscattered to the copper atom, thus suggesting a type of "cage effect" at the low electron energies associated with the XANES region.

These calculations, and those shown in Figure 4a, show that the XANES spectra are sensitive to the relative orientation of the imidazole rings. This insight offers the possibility that the relative orientation of different residues around a metal site can be investigated by using high-resolution XANES spectra, particularly when strong multiple scattering may occur from the atoms of such ligands. Figure 4a shows reasonable agreement with the experimental data (Figure 4b) for most of the features with respect to their relative position; however, the relative amplitudes of these features are not as well reproduced. This problem is known to be associated with the general one of calculating accurate phase shifts for the low-energy scattering regime. Thus, it is likely that a more accurate method of calculating phase shifts is required if the recent advance in XANES theory is to be fully exploited. Self-consistent field methods of calculating atomic potentials may prove useful in this respect. On the other hand, genuine many-electron excitations may also be occurring; in general, such effects lie beyond a single-particle scattering approach. In this instance, the strength of many-electron effects seems to be quite small but may complicate the quantitative details of the analysis. We also note that such detailed understanding is only feasible if the nature and position of ligands are well-defined from other methods, such as crystallography and EXAFS. It is also important that XANES profiles are compared within a related family of compounds, as similar features may be observed from chemically unrelated systems due to similar backscattering paths.

Conclusion

A detailed investigation of the XANES of a family of Cu(II) imidazole complexes has shown that the spectral features observed for this class of compounds can be understood in terms of electron-scattering theory. The potential for extracting useful stereochemical information from the XANES has been demonstrated.

Acknowledgment. We thank the Science and Engineering Council for their support of this work. We are also thankful to several of our colleagues, particularly to Drs. N. J. Blackburn and C. D. Collison and Professor C. D. Garner for their support and useful discussions. Dr. Blackburn and Professor Garner also supplied the protein and chemical compounds, respectively.

Rotational Reorientation of the 1-Adamantyl Cation: A Sensitive Probe of Carbocation–Medium Interactions

David P. Kelly* and D. Ralph Leslie†

Contribution from the Department of Organic Chemistry, The University of Melbourne, Parkville, Victoria, Australia 3052. *Received October 10, 1989*

Abstract: Rotational reorientation of the 1-adamantyl cation has been determined over a range of temperatures (−90 to −40 °C) and concentrations (0.21–0.69 M), of the cation generated from different precursors (ROH, RCl) in different superacids (SbF_5, FSO_3H/SbF_5) with different solvents (SO_2, SO_2ClF). The anisotropy of reorientation, as measured by the ratio of the diffusion constants ($\sigma = D_\parallel/D_\perp$), was independent of precursor, temperature, and concentration, but not the solvent. In SO_2 solution the cation reorients isotropically ($\sigma = 1$) but anisotropically ($\sigma = 2.5$) in SO_2ClF. This anisotropy is considered to arise from weak electrostatic interactions of the cationic center with a diffuse anionic "cloud" in the medium and not from ion pair formation. These results are in contrast to those from thermochemical studies.

The study of carbocations as stable, long-lived species was made possible by the discovery of the liquid superacids, in particular SbF_5, FSO_3H, and "Magic Acid".[1] The very existence of stable carbocations in these acids attests to the very low nucleophilicity of the acids, their conjugate bases, and the counterions generated during cation formation. While there is now a large body of literature dealing with the structure of the carbocations in superacid media,[1-3] there has been relatively little investigation of

†Current address: Materials Research Laboratory, DSTO P.O. Box 50, Ascot Vale, Victoria, Australia 3052.

(1) Olah, G. A.; Surya Prakash, G. K.; Sommer, J. *Superacids*; Wiley Interscience: New York, 1985.

0002-7863/90/1512-4268$02.50/0